Experimental Neurology 398 (2026) 115639

Contents lists available at ScienceDirect

Experimental Neurology

journal homepage: www.elsevier.com/locate/yexnr

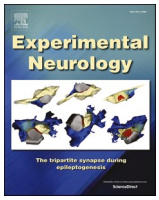

Research paper

# Daily intranasal resveratrol-conjugated gold nanoparticles administration promotes neuroprotection and improves neurological outcome in the R6/2 mouse model of Huntington's disease

Emanuela Paldino [a,b], Emiliano Montalesi [c], Marco Fiocchetti [c,d], Flavia Dioguardi [a,e], Iole Venditti [c,d], Elena Olivieri [c], Maria Marino [c,d], Francesca R. Fusco [a,*]

[a] Laboratory of Neuroanatomy, IRCCS Santa Lucia Foundation, Via del Fosso di Fiorano 64, 00143 Rome, Italy
[b] Department of Health Sciences, Link Campus University, Via del Casale di San Pio V, 44, 00165 Rome, Italy
[c] Department of Science, University Roma Tre, Viale Guglielmo Marconi 446, 00146, Rome, Italy
[d] Laboratory of Neuroendocrinology, metabolism and neuropharmacology, IRCCS Santa Lucia Foundation IRCCS Santa Lucia Foundation, Via del Fosso di Fiorano 64, 00143 Rome, Italy Rome, Italy
[e] Department of Psychology, Sapienza University of Rome, Via dei Marsi 78, 00185, Rome, Italy

ARTICLE INFO

*Keywords:*
Huntington's disease
Neuroinflammation
Drug delivery
Resveratrol
Nutraceutical strategy
Preclinical research

ABSTRACT

Pan-apoptosis and involvement of the inflammatory process are the hallmarks of Huntington's disease (HD). Inflammation currently represents one of the potential therapeutic targets for slowing and fighting the pathological phenotype of HD. The immunomodulatory properties of natural compounds, such as resveratrol, have been demonstrated in various disease models and human clinical trials. In the present study, we evaluated the neuroprotective and anti-inflammatory effects of the daily intranasal administration of resveratrol-conjugated gold nanoparticles in awake R6/2 mice, the genetic animal model of HD. Transgenic mice were treated daily with resveratrol-conjugated gold nanoparticles (0.1 mg/kg/day) starting from 5 weeks of age corresponding to the prodromal stage of the disease. After sacrifice, histological and immunofluorescence studies were performed. We found that resveratrol treated R6/2 mice survived longer and displayed a significant partial recovery of motor performance compared with R6/2 mice that received the nanoparticles with vehicle. Primary outcome measures such as striatal atrophy, neuronal intranuclear inclusions, and modulation of microglial reaction revealed a neuroprotective effect of resveratrol conjugated gold nanoparticles. Resveratrol provided a significant increase of neuroglobin, a neuroprotective globin, along with activated CREB and BDNF in the mice medium spiny neurons, accompanied by a down modulation of neuroinflammation, which, combined, might explain the beneficial effects observed in this model. Our findings showed that nanoparticles loaded with a specific compound which acts on the mutated protein intranuclear inclusions and inflammatory components may represent a valid therapeutic strategy in slowing down the symptoms of HD neurodegeneration.

## 1. Introduction

Huntington's disease (HD) is a rare and progressive genetic disease characterized by the irreversible damage of neuronal cells. The expansion of polyglutamine (polyQ) tract determined by the autosomal mutation of the gene coding for the huntingtin protein causes a massive loss of striatal neurons (MacDonald, *1993*; Vonsattel and DiFiglia, *1998*) and consequently cognitive and motor coordination dysfunction. Neuronal intranuclear inclusions (NIIs), derived by mutated huntingtin protein (mHTT), promote the main clinical symptoms of disease interacting and interfering with several intracellular proteins that regulate the metabolic and physiological processes of neurons. Moreover, mHTT protein results in a pro-inflammatory activation of microglia which influences disease onset and progression (Crotti et al., *2014*). In particular, the expression of inflammatory cytokines and biomarkers produced by pro-inflammatory microglia has been described in the brains of HD patients, suggesting that central and peripheral inflammation represent a critical phase in the progression and amplification of HD pathology (Yang et al., 2017).

Currently, there is not a specific cure for this disease, although

* Corresponding author.
*E-mail address:* f.fusco@hsantalucia.it (F.R. Fusco).

https://doi.org/10.1016/j.expneurol.2026.115639
Received 3 September 2025; Received in revised form 24 December 2025; Accepted 6 January 2026
Available online 7 January 2026

genetic clinical trials are underway to prevent the production of mutated protein. However, given the role of inflammation in worsening the disease's symptoms, basic research and the pharmaceutical industry are working together to identify new target molecules or to repurpose drugs already in clinical use. For this purpose, emerging anti-inflammatory approaches have been developed, aimed at reducing neuro-inflammation by supporting the resistance of striatal neurons to the degenerative process (Paldino et al., *2020a, 2020b;* Thomas et al., *2004;* Bouchard et al., *2012*).

Resveratrol (Resv) is a polyphenolic compound in various plants, including grapes, peanuts, and berry fruits, which is celebrated for its several health benefits such as anti-obesity, cardioprotective, neuro-protective, antitumor, antidiabetic, antioxidants, anti-age effects, and glucose metabolism (*Fulda, 2010a, b*).

The chemical structure of resveratrol (trans-3,5,4′-trihydroxystilbene) has been identified in two isomers: *cis*-Resv and *trans*-Resv. In Resv the hydroxyl groups in the 3, 4′, and 5 positions are main factors in the antioxidant activity against hydroxyl (·OH) and hydroperoxyl (·OOH) radicals in aqueous (Cracco et al., *2023;* Venditti et al., *2020*). However, these effects are reported in cell lines at very high concentration of Resv (i.e., 10 mM). In addition, Resv at concentrations ranging from 0.1 to 1 mM has a significant role in enzyme and pathway modulation. Among different mechanisms underlying neuroprotective effect (e.g. inhibition of NF-kB and the induction of SIRT-1 pathways), Resv modulates the activity of estrogen receptor beta subtype (ERβ), increasing the level of a neuroprotective protein, neuroglobin (NGB) that reduces oxidative stress and increases cell resilience against apoptosis (Montalesi et al., *2023*).

The chemical structure of polyphenols reduces their solubility, increasing their biotransformation, which affects the bioavailability of these compounds, thereby limiting their therapeutic use (Zhang et al., *2021*). The landing of nanotechnology in preclinical research and, specifically, the use of nanoparticles as carriers could reduce these natural limitations, increasing the bioavailability of polyphenols, and their effectiveness. Recently, Resv conjugated with gold nanoparticles has been efficiently synthesized and characterized in terms of toxicity and NGB modulation in breast cancer cells and neuronal-derived cells. Results indicate that gold nanoparticles enriched with Resv significantly increase NGB level already at concentration of 10 nM protecting cells against oxidative stress-induced apoptosis (Venditti et al., *2020;* Montalesi et al., *2023*).

In our study, the primary objective was to investigate neuroprotective effects of resv achieved by a prolonged administration of Resv conjugated-AuNPs to the R6/2 mouse model of HD. The therapeutic strategy consists of a gold core and a dense, packed shell of Resv. This kind of packed distribution prevents Resv biodegradation, improving their pharmacokinetics and enhancing the therapeutic effect. To overcome the bioavailability problems of the natural compound, Resv-AuNPs were administrated daily to awake mice.

Our results show that Resv-conjugated AuNPs efficiently target mice striatum promoting a selective effect on mutated protein aggregation. Moreover Resv-AuNPs promote mice survival and improves R6/2 motor coordination. The nanoparticle is a promising mean of delivery for drugs that do not cross the BBB and tend to be degraded promptly.

## 2. Materials and methods

### 2.1. Synthesis and Purification of AuNPs and Resv conjugated-AuNPs

The gold AuNPs stabilized with citrate and L-cystein (L-cys) were prepared and characterized in analogy to literature reports (Venditti et al., *2020*). Briefly: 25 mL of L-cys solution (0.002 M), 10 mL of cit solution (0.01 M), and 2.5 mL of tetrachloroauric acid solutions (0.05 M) were mixed sequentially in a 100 mL flask, provided with a magnetic stir. After degassing with Argon for 5 min, 4 mL of sodium borohydride solution (0.00008 M) was added, and the reaction continued for 2 h at room temperature. Then, the solid brown product was purified by centrifugation (13,000 rpm, 10 min, 4 times with deionized water). AUNP-R synthesis was carried out following the same procedures but including Resv water solution (1 mL 0.02 M) in the reagent mixture, before reduction.

### 2.2. The genetic animal model of Huntington's Disease

All animal experiments, which satisfy ARRIVE guidelines, were performed in accordance with European Communities Council Directive (2010/63 EU) as adopted by the Santa Lucia Foundation Animal Care and Use and approved by Italian Ministry of Health. Transgenic female R6/2 mice carrying the mutant human HTT exon 1 were kept in coupling with B6CBAF1/J males, all obtained from Jackson Laboratories (Bar Harbor, ME). Animals were pathogens free, including common pathogens such as Helicobacter. F1 mice were used to perform all experiments. Standard PCR was performed to genotype animals at 21 days of age, subsequently mice were weaned, and the treatment started.

### 2.3. Methodology and technique for the intranasal administration to awake mice

All experimental mice were acclimated to handling for a period of two weeks before the onset of intranasal dosing. Animals' acclimation is a very important step because it ensures a correct body position for maximum effectiveness of awake intranasal Resv-AuNP delivery. Mice stress response level, such as movements, the amount/frequency of urination, defecation, trembling, and biting were monitored before treatment until the response was reduced. Treatment started at 5 weeks of age. A detailed description of the method of intranasal administration is described in supplementary material n.3. Wild type (Wt) and R6/2 mice (8 mice/per experimental group) were treated with either vehicle (AuNP) or Resv-conjugated AuNP (0.1 mg/kg/day). Animals were identified by a randomly assigned code and housed 4 per cage under conventional laboratory conditions (room temperature 20 ± 2 °C; humidity 60%) and a 12/12 h light/dark cycle (7:00 am–7:00 pm) with ad libitum access to food and water. All the experimental data were collected by observers who were blinded to genotypes and treatment (Fig. 1).

### 2.4. Survival and weight

The survival study was conducted following the criteria for euthanasia (Hersch and Ferrante, *2004*), which is the point when R6/2 could not right themselves after 30s when placed on their side. This point is usually reached by vehicles treated R6/2 mice at 11/12 weeks of age. However, R6/2 mice treated with Resv-AuNPs showed greater survival around 14/15 weeks of age. WT mice survive longer, and for a reliable statistical comparison, we chose the 14th week of age. All experimental mice were weighed twice a week starting from the beginning of treatment until sacrifice. Their weight was recorded, and weight variations were calculated and plotted.

### 2.5. Stereological analysis of gross striatal area and neurons survival

Paraformaldehyde-perfused mice brains were removed and placed in a sucrose (20%) and glycerol (10%) in PB 0.1 M solution. After precipitation, brains were frozen in liquid nitrogen and prepared for cryostat sectioning. Standard Nissl staining was performed on coronal step serial sections from rostral neostriatum through the level of anterior commissure (interaural 4.66 mm/bregma 0.86 mm to interaural 3.34 mm/bregma −0.14 mm) from 8 animals per group. Gross striatal area was measured using Neurolucida™ Stereo Investigator software (MBF bioscience, Williston, VT, USA) running the Cavalieri estimator probe.

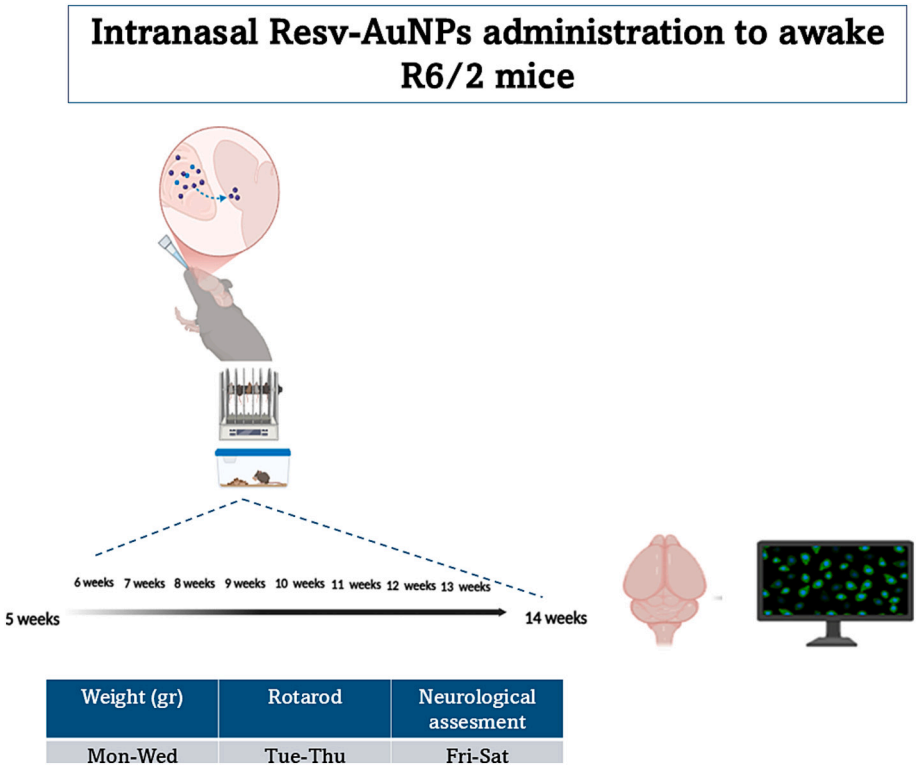


**Fig. 1.** The primary stages of this research include the Resv-conjugated gold nanoparticles production process, the chronic intranasal administration to awake mice, and the evaluation of the neuroprotective properties exhibited by resveratrol (graphical experimental abstract was obtained by **Biorender** digital software). (For interpretation of the references to colour in this figure legend, the reader is referred to the web version of this article.)

### *2.6. Analysis of mutated huntingtin intranuclear inclusions*

Brain sections taken with the same stereotaxic coordinates (interaural 4.66 mm/bregma 0.86 mm to interaural 3.34 mm/bregma −0.26 mm) were processed for single label EM-48 ubiquitin (Chemicon, Temecula, CA) immunofluorescence and counterstained with NeuN (rabbit anti NeuN-ABN78) to calculate the number of neurons containing intranuclear inclusions (NIIs). The nucleus of each neuron was examined to ascertain the presence of NIIs. All neurons in each hemisphere for each brain section of all mice were analyzed to determine the number and size of NIIs in the striatal neurons in both vehicle (empty AuNPs) and Resv-AuNPs-treated R6/2 mice (wild-type littermates did not show NIIs–like ubiquitin immunoreactivity). Images were acquired with a 40× and 63× objective on a confocal laser scanner microscopy (Zeiss LSM 800) under no saturating exposure conditions. The same acquisition setting was performed for each sample.

### *2.7. Microglial morphology*

Microglial morphology was studied by immunostaining brain sections with antibody labeling microglia (1:500 goat anti-Iba-1 from Novus Biological, Italy). Striatal brain sections were incubated with the primary antibody for 72 h at 4 °C, followed by incubation with the secondary antibody for 2 h at room temperature. Immunofluorescence images were acquired with confocal laser scanner microscopy (Zeiss LSM 800) in order to perform morphology analysis. Microglia cells were captured using a 40× objective producing images in the format 1024 × 1024, and Airy Units 1.0. This configuration was used for all samples. Collected images were exported in TIFF format, brightness and contrast were adjusted. The protective or toxic phenotype was characterized by using *Z*-stack images, performing the Sholl analysis.

### *2.8. Immunofluorescence and confocal microscopy studies*

Brain tissue sections were incubated with primary antibodies for 72 h at 4 °C, followed by incubation with secondary antibodies for 2 h at room temperature. Neurons were counterstained for their visualization with Neurotrace™. The primary antibodies used were anti-pCREB (1:200 polyclonal pCREB, Millipore, Italy), BDNF (1:200 polyclonal anti-BDNF, Novus Biologicals, Italy), NGB (1:600 anti-Neuroglobin, Merck Millipore, Darmstadt, D), and CALB (1:100 mouse anti-Calbindin, Novus Biologicals, Italy). The secondary antibodies used were Alexa Fluor 488 and Alexa Fluor 555 (Immunological Science). Brain sections were mounted on gelatin- coated slices, cover slipped with gel-mount. Samples were examined with the support of confocal laser scanner microscopy (Zeiss LSM 800), images were acquired and subsequently analyzed to quantify the immunofluorescence intensity.

### *2.9. Mice behavior*

#### *2.9.1. Rotarod*

The five-station rotarod performance test (Rotarod/RS LSI Letica, Biological Instruments, Varese, Italy) was used to estimate mouse motor coordination and balance. Tests were performed by placing mice on a horizontally rotating rod, which is low enough to prevent animal damage, but high enough to induce the fall. Mice performed rotarod test twice weekly from 4th to 13/14th weeks of age. Three trial sessions of 60 s each were performed at a constant speed of 15 rpm, and the latency to fall from the rod was recorded. A maximum latency of 60 s was defined for mice that did not fall.

### *2.10. Statistical analysis*

Statistical analysis was performed by ANOVA available on the software Stat 5 and GraphPad Prism version10.0. $p$ values $<0.05$ were

considered statistically significant. Survival data were analyzed by means of a product limit method of Kaplan and Meier and *p* value was set at 0.001 for significant results. Regarding the behavioral analyses, a three-way ANOVA was performed to evaluate the effects of genotype, age, and treatment. Quantitative analyses of immunofluorescence signal intensity were carried out using the Friedman test, and post-hoc comparisons were performed using the Wilcoxon signed-rank test with Šidák correction. For the immunofluorescence assessments, serial sections from each subject within the experimental groups were analyzed. Cells of interest were selected using the circle selection tool. From the *Analyze* menu, the "Set Measurements" function was used to select "Mean Grey Value," "Area," and "Min & Max Grey Value." The region adjacent to the cells, showing no fluorescence, was defined as the background and subtracted. Finally, the *Measure* command from the *Analyze* menu was applied to obtain mean values. Mean values and corresponding standard deviations were calculated, and graphical representations were

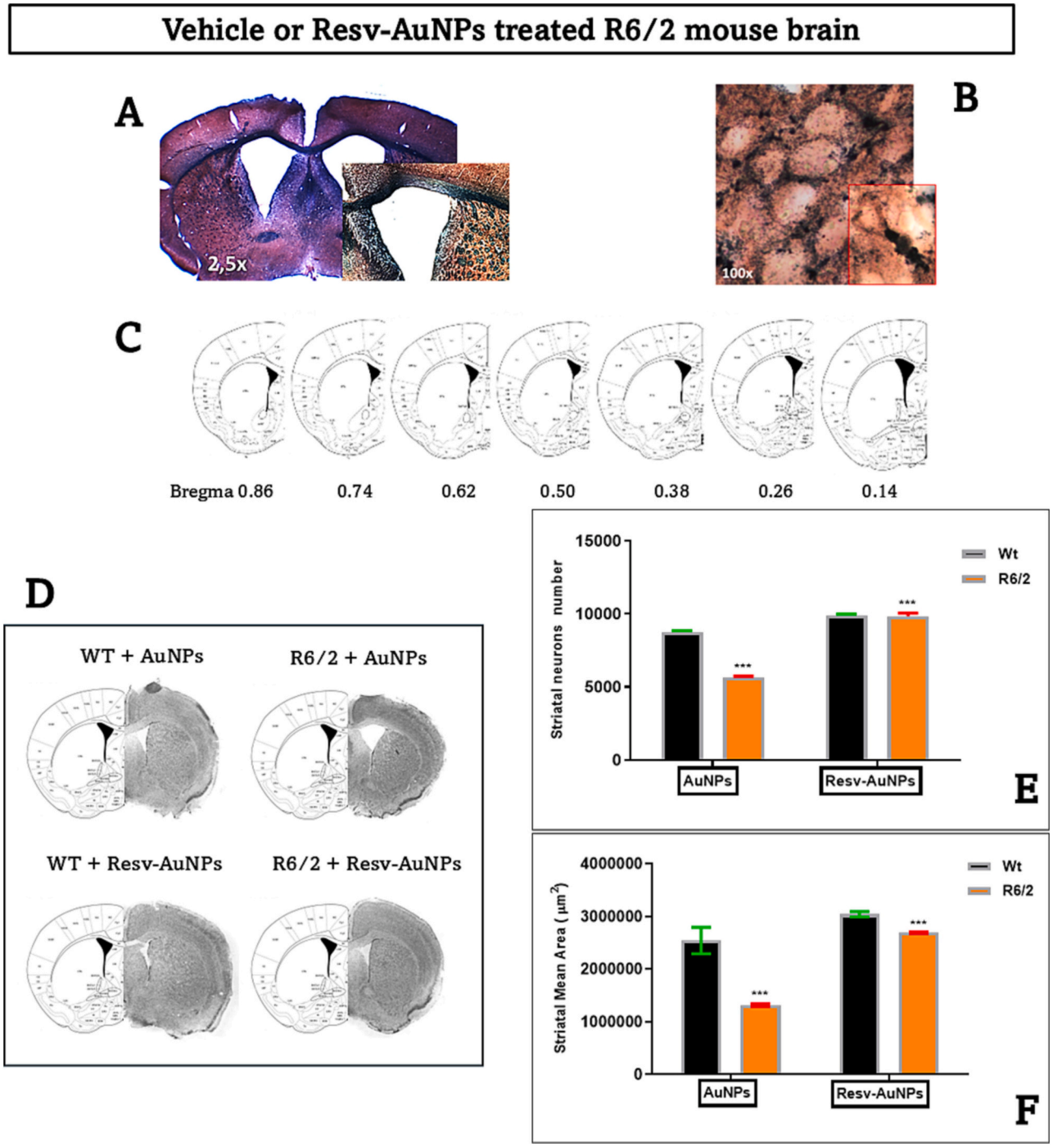


**Fig. 2.** Intranasal treatment with Resv-AuNPs reduced striatal atrophy in R6/2 mice. Gold nanoparticles were visualized to confirm their presence within the target tissue. *Nanogold Staining*™ revealed that nanoparticles successfully reached the striatum of 14-week-old mice following intranasal administration (A–B). (D) Representative transmitted light micrographs show Nissl-stained coronal sections from Wt and R6/2 mice treated with either vehicle-AuNPs or Resv-AuNPs. R6/2 mice treated with vehicle-AuNPs exhibited pronounced striatal atrophy and ventricular enlargement compared with those treated with Resv-AuNPs. (*E*-F) Histograms represent mean ± SEM values for striatal neuron counts and area quantification. Two-way ANOVA revealed a statistically significant effect of treatment on striatal neuron survival. (For interpretation of the references to colour in this figure legend, the reader is referred to the web version of this article.)

generated using GraphPad Prism (version 10).

## 3. Results

### 3.1. Intranasal Resv-AuNPs administration attenuates neuropathological changes in R6/2 Mice

#### 3.1.1. Stereological analysis of experimental mice brains

Nanogold staining™ revealed that the nanoparticles had reached the

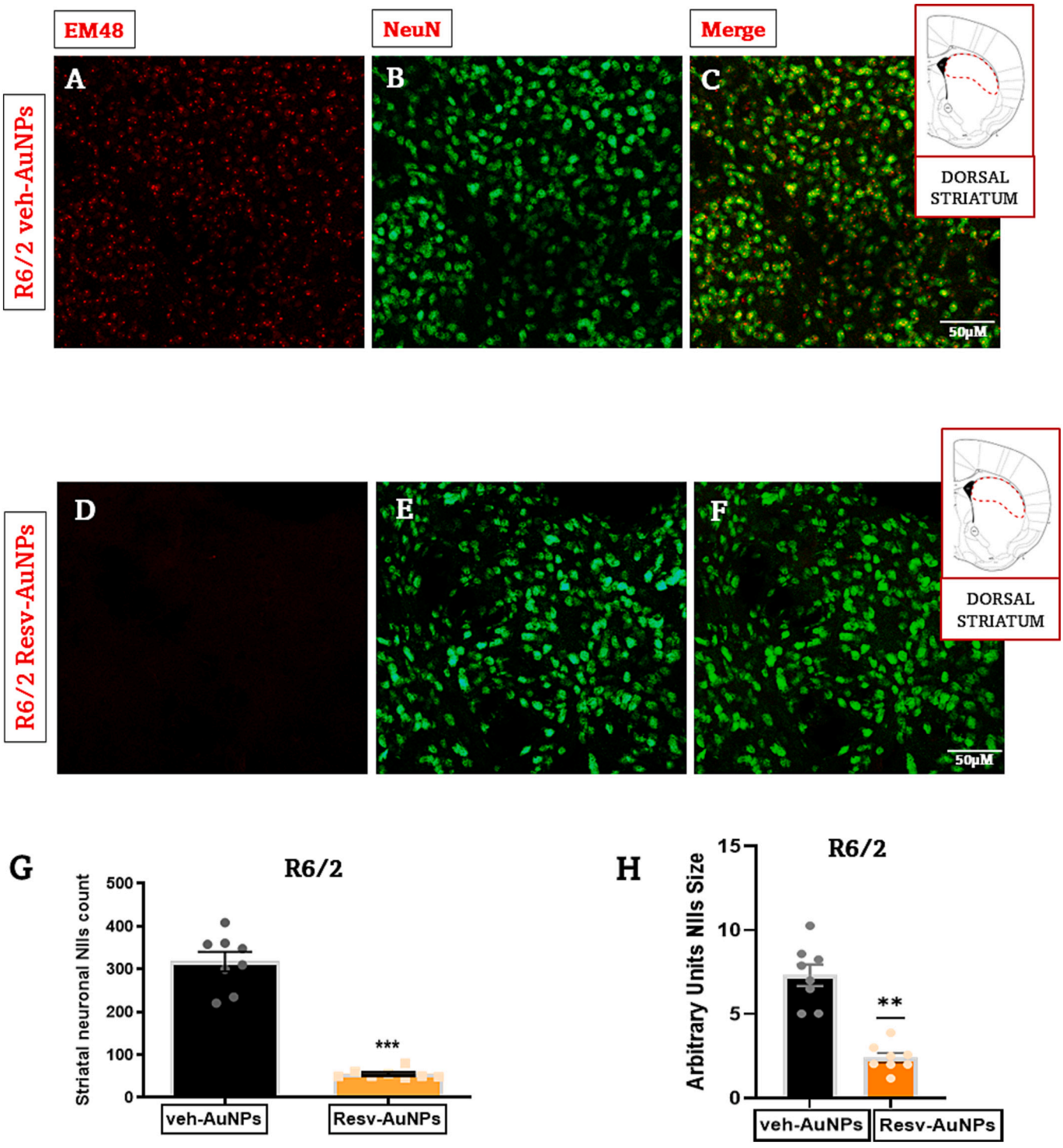


**Fig. 3.** Resv-AuNPs treatment reduces NIIs number and size in R6/2 mice. Statistical analysis performed on data obtained by veh-and Resv-AuNPs-treated R6/2 mice (4 brain sections for mice) revealed a statistically significant effect of treatment on NIIs number and size. White panels illustrate the dorsal striatal region at the corresponding stereotaxic coordinates, highlighting the area where the reduction in NIIs is most evident.(G-H) histograms show a significant decrease of NIIs number and size in mice treated with Resveratrol respect to empty AuNPs-treated R6/2 mice.

striatum of empty or Resv-AuNPs treated R6/2 through intranasal administration (Fig. 2A-B). Stereology analyses showed that the striatal area of empty AuNPs-treated R6/2 mice was smaller than WT animals (with an average area of 1318 $\mu m^2$ compared to 2600 $\mu m^2$ of the wild-type littermates). Treatment of R6/2 mice with Resv-AuNPs prevented striatal area reduction (2691 $\mu m^2$) [$F_{1,28} = 53.27$ $p = 0.001$]. (Fig. 2C). Empty or Resv conjugated AuNPs did not produce any statistically significant changes in the WT control group. The preventive reduction of R6/2 striatal area was due the greater neurons survival as highlighted by stereological count. The estimated population of intranasal Resv-AuNPs treated mice was 9857 $\times 10^5$ $\mu m^2$ compared to 5658x$10^5$$\mu m^2$ calculated on vehicle-AuNPs treated R6/2 [($F_{1,28} = 1245$ $p < 0.001$), treatment ($F_{1,28} = 3507$; $p < 0.001$) and genotype $\times$ treatment interaction $F_{1,28} = 1157$; $p < 0.001$)].

### 3.2. *Resv-AuNPs reduced NIIs in the R6/2 striatal neurons*

The expression of mHTT in the R6/2 mice promotes the formation of

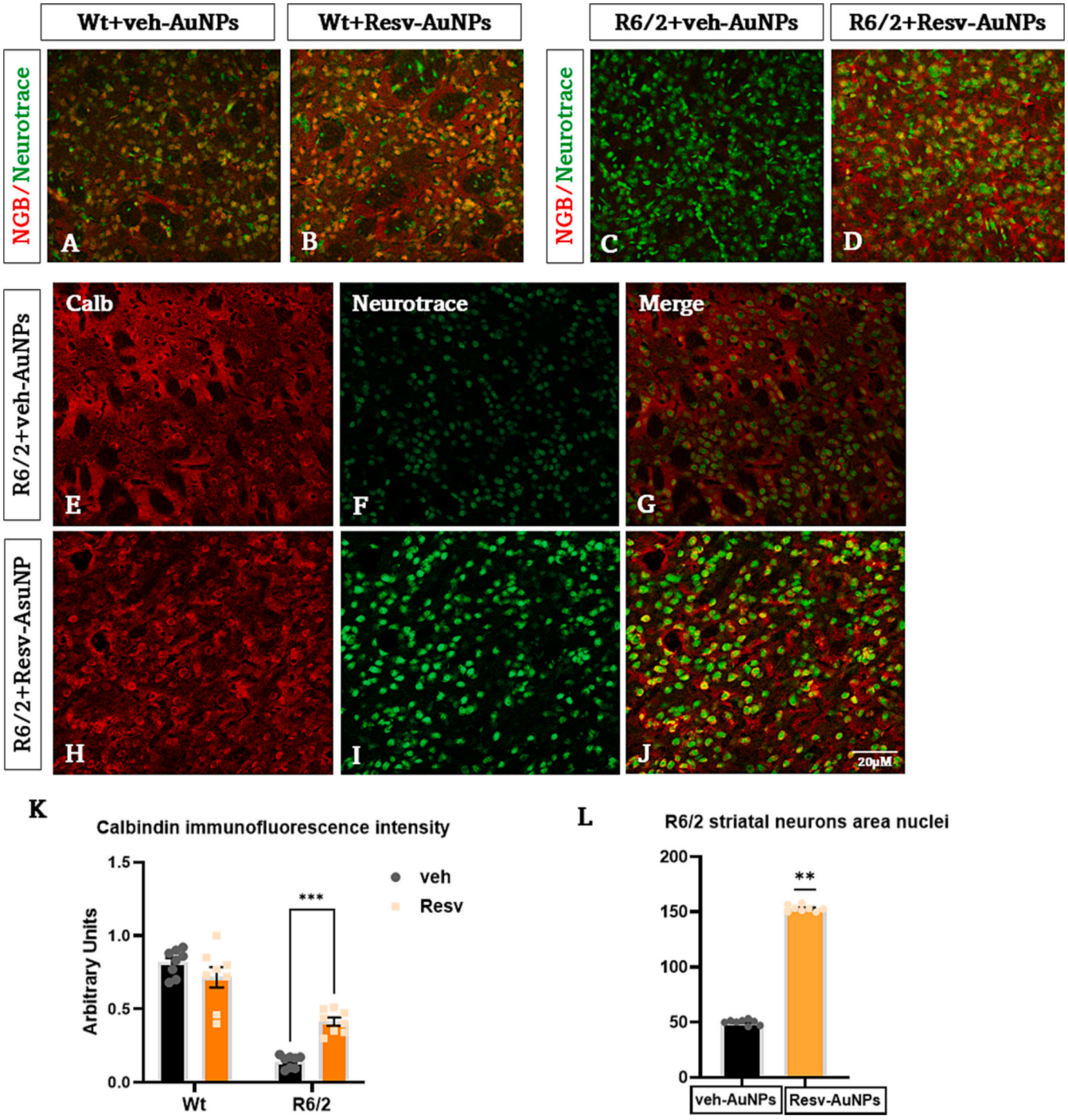


**Fig. 4.** (A-D) Resv-AuNPs promotes NGB expression and striatal medium spiny neuroprotection in R6/2 mice. Images are confocal laser scanning microscopy acquisitions of double-label immunofluorescence for NGB and Calb (visualized in red-Cy3 fluorescence) and the Nissl-like fluorescent marker Neurotrace (visualized in green fluorescence). (E-J) collected images show the effect of intranasal Resv-AuNPs administration in R6/2 mice striatal neurons (K) Histograms show Calbindin quantification with a significant effect of Resv-AuNPs, highlighting a greater atrophy of neurons nuclei area in promoting neuronal protection(L). (For interpretation of the references to colour in this figure legend, the reader is referred to the web version of this article.)

neuronal intranuclear inclusions (NIIs) detected with the antibody EM-48. The analysis of EM-48 immunofluorescence in the striatal brain region of 14-week-old R6/2 mice treated with Resv, counterstained with NeuN showed that the number of NIIs was significantly reduced compared to the empty AuNPs-treated group. NIIs reduction was evident especially in correspondence with the dorsal striatum, the brain region mainly involved in the neurodegenerative process due to its close proximity to the cortical region (Fig. 3 A-D). Moreover, the analysis of all Resv-AuNPs treated R6/2 mice revealed that the area of NIIs decreased compared to that of control mice (3H). This significant reduction in the number ($p < 0.001$) and size ($p$ ⟨0,001) of EM-48 immunoreactive NIIs confirmed that the daily intranasal Resv-AuNPs administration, starting from the pre symptomatic stage of the disease, strongly reduced and delayed the development of neuronal inclusions in R6/2 mice.

### 3.3. *Resv-AuNPs promoted the NGB overexpression in striatal neurons of R6/2 mice*

Resv is a potent inducer of neuroglobin expression. The R6/2 mice do

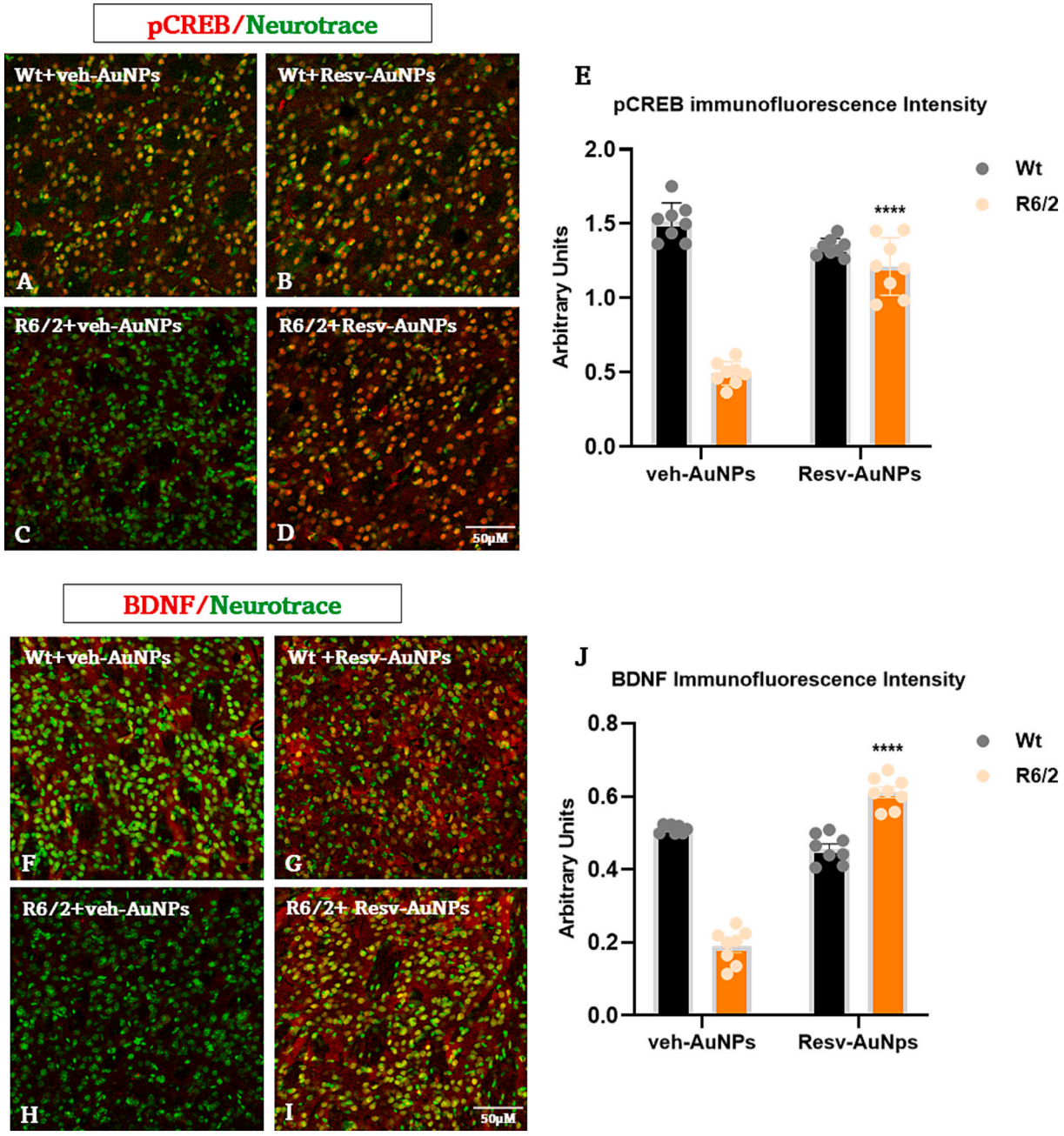


**Fig. 5.** Effects of Resv-AuNPs daily intranasal administration on CREB and BDNF activation. Representative confocal laser scanning microscopy images of dual label immunofluorescence for pCREB (red) and Neurotrace (green) in striatal samples from a veh-AuNPs treated wild type (A), Resv-AuNPs treated wild type (B), veh-AuNPs treated R6/2 (C) or R6/2 treated with Resv-AuNPs (D). E: Histograms show the intensity of immunofluorescence of pCREB in the Resv- treated R6/2 mice. R6/2 mice treated with vehicle AuNPs had a significantly reduced pCREB level compared to the vehicle treated wild type group. pCREB levels were higher in R6/2 animals treated with Resv-AuNPs compared to the vehicle treated R6/2 animals. (F—I) R6/2 mice treated with vehicle AuNPs had a significantly reduced BDNF level compared to the vehicle treated wild type group and there was no statistically significant difference in BDNF level wild-type mice treated with Resv-AuNPs or vehicle. In this case also, BDNF levels were higher in R6/2 animals treated with Resv-AuNPs compared to vehicle treated R6/2 animals, as shown in the histogram (J). (For interpretation of the references to colour in this figure legend, the reader is referred to the web version of this article.)

not express sufficient levels of this protein which correlates with the worsening of the neurodegenerative process (Cardinale et al., *2018*). We verified the neuroprotective effects of Resv-AuNPs also evaluating the expression of neuroglobin. The representative immunofluorescence images confirmed that in the empty AuNPs- treated R6/2 mice the expression of neuroglobin is very low. The expression was significantly up- regulated in the R6/2 mice treated with Resv-AuNPs. The same effect was also observed in the WT littermates even though they presented a basal expression of neuroglobin. The reduction of NIIs inclusions and the modulation of neuroglobin expression correlated with the maintenance of calbindin expression (Fig. 4K). This was linked to the survival of medium spiny neurons that selectively degenerate in HD disease ($p < 0.001$). Moreover, the analysis conducted on the neuron's morphology highlighted a greater atrophy of neurons nuclei area of Resv-AuNPs treated mice compared to animal control, suggesting an increase in protein synthesis as a cellular adaptation to the in-situ treatment (Fig. 4L) ($p < 0,001$).

### 3.4. *Resv-AuNPs prevented CREB and BDNF expression reduction in R6/2 mice*

We investigated the effect of Resv-AuNPs intranasal treatment on CREB and BDNF protein expression in the striatum of R6/2 mice. Resv-AuNPs treated R6/2 mice displayed a significantly higher expression of phosphorylated CREB (pCREB) in the surviving spiny neurons of R6/2 mice (Fig. 5 A-D). The intensity of pCREB, expressed in arbitrary units,

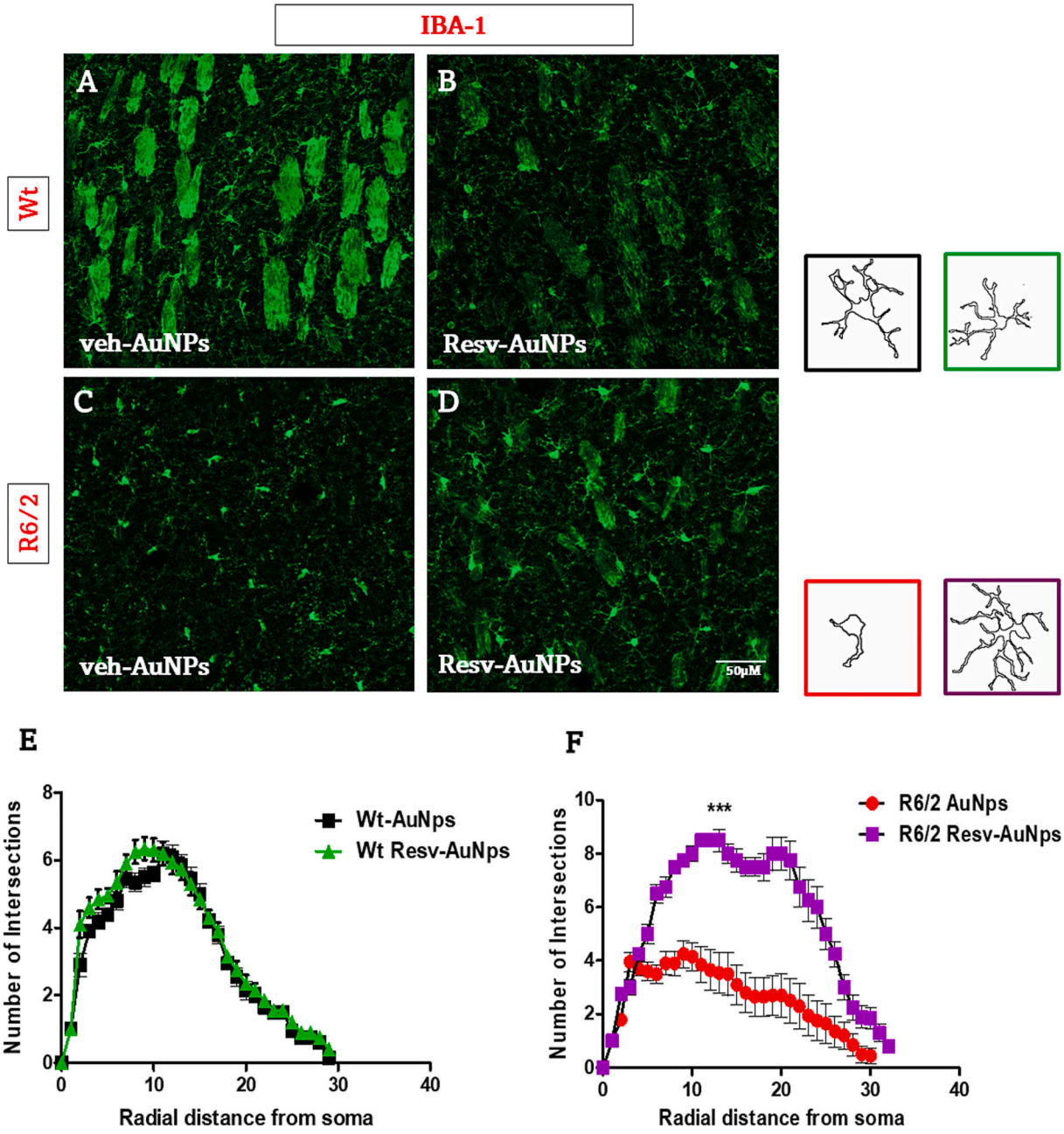


**Fig. 6.** Daily intranasal Resv-AuNps administration reduces microglial activation. a Representative confocal image showing the distribution of microglia in all experimental groups ($n = 8$ for each group; 3 brain sections for mice). Lower microglia activation was recorded in the Resv-AuNPs-treated R6/2 mice with respect to the R6/2 control group. Sholl analysis revealed a significant increment of microglia intersections number in the R6/2 mice treated with resveratrol compared to vehicle AuNPs treated R6/2 mice suggesting a significant reduction of phenotypic ameboid microglial positive cells. Boxed images display representative Iba-1–positive cells from each of the four experimental groups, which were converted into binary format for Sholl analysis.

was, indeed, significantly lower in the control R6/2 mice compared to Wt littermates. BDNF is a CREB target gene (*Giampà* et al., *2006a, b*; Paldino et al., *2017*; Zuccato et al., *2001*), therefore we aimed at verifying if the above-described increase of pCREB was associated with an upregulation of BDNF. As shown in Fig. 5H, Resv-AuNps treated R6/2 mice showed a significantly higher BDNF protein expression, compared to R6/2 mice receiving empty-AuNPs (Fig. 5G) The daily intranasal Resv AuNPs administration was, therefore, effective in preventing the well described loss of BDNF in HD (Zuccato et al., *2001*; Fusco and Paldino, *2024*). Two-way ANOVA indicated a significant effect of genotype $F1,28 = 324.5$; $p < 0.0001$, a significant treatment effect $F1,28 = 191.0$; $p < 0.0001$ and a significant genotype × treatment interaction $F1,28 = 39.61$; $p < 0.0001$.

### 3.5. Resv-AuNPs treatment reduced Microglia activation in R6/2 mice

Iba-1 immunofluorescence was performed to address the different activation stages of microglia. Wt mice treated with AuNPs or with Resv-AuNPs displayed a ramified or primed microglia which shows a bigger cell body. The presence of active Iba-1 positive cells in the AuNPs treated Wt mice is attributed to the nanoparticles that induce a physiological response of the resident cells of the immune system because the chronic treatment with empty or Resv AuNPs can induce a partial state of inflammation (Fig. 6B). The immunostaining for Iba-1 in the R6/2 control group revealed an intense microglial reaction, where numerous microglial cells appeared and displayed an amoeboid cell body in which there are still present few ramified or unramified processes (Fig. 6C). Microglial reaction appeared attenuated in Resv-AuNPs treated R6/2 mice, with fewer reactive Iba-1 positive cells and a smaller circular cell body with a ramification pattern that suggests a resting phenotype ($F_{1,24} = 9.747$ $p < 0.001$)(Fig. 6D).

### 3.6. Intranasal Resv-AuNPs administration increases R6/2 Mouse Survival and Motor Performance

Resveratrol treatment promoted a longer survival of R6/2 mice, as shown by the Kaplan-Meier curve. In our study, R6/2 mice were followed weekly until death. R6/2 control mice, expressed as a percentage of survival, died between days 77 and 84, whereas Resv AuNPs- treated R6/2 survived 2 weeks longer as shown in Fig. 7A. Motor behavior performances of mice were evaluated by rotarod apparatus. R6/2 mice had a statistically significant impairment in motor coordination compared to Wt mice $p < 0.001$; the three-way ANOVA showed a significant improvement of motor performance $p < 0.001$ after intranasal Resv-AuNPs treatment in R6/2 mice (7B).

## 4. Discussion

Our data show that the intranasal administration of resveratrol is protective in the R6/2 mouse model of HD in terms of survival, motor performance, and neuroprotection. The positive effects induced by Resv-AuNPs were associated with a significant decrease in the nuclear inclusions formation.

At a neuropathological level, we found that Resv-AuNPs significantly

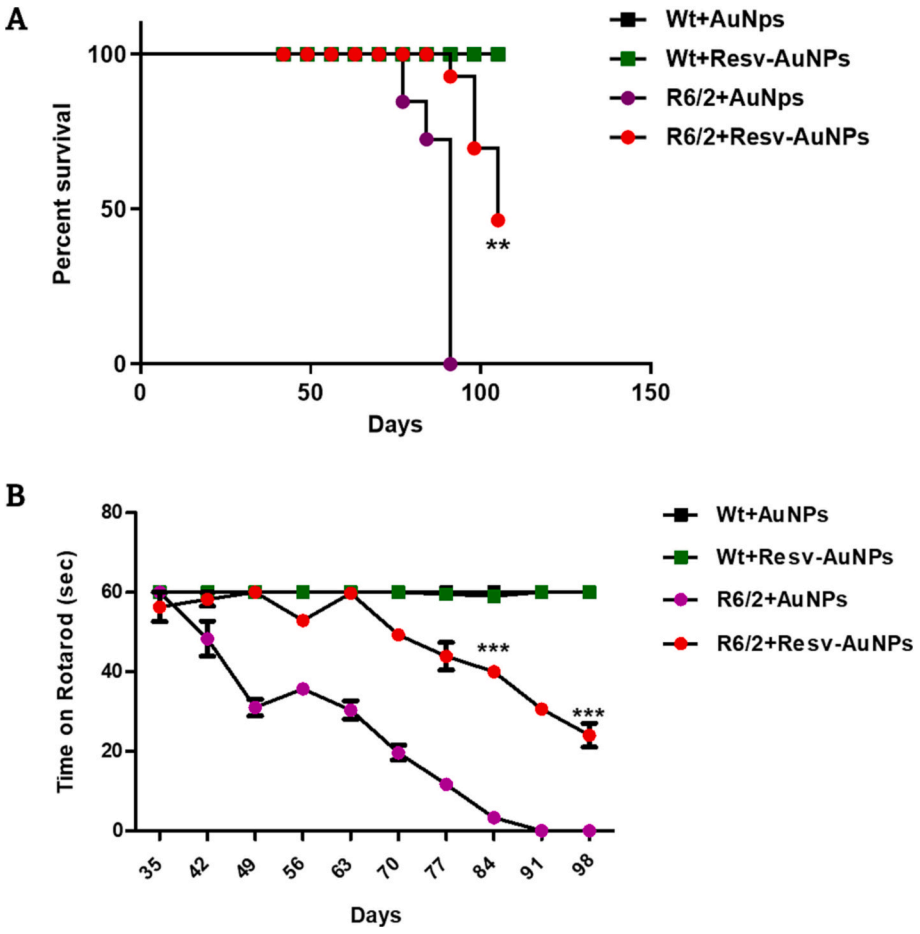


**Fig. 7.** Survival and motor performance of R6/2 mice treated with Resv-AuNPs. (A) Kaplan-Meier curve of survival showed that R6/2 mice treated with Resveratrol had a mean survival time significantly ($p < 0.001$) longer than that of R6/2 mice control group. **(B)** A three-way ANOVA with genotype, treatment and time as main factors, revealed that R6/2 mice have a statistically significant impairment in motor coordination respect to wild-type mice and that Resv-AuNPs intranasal treatment improves performance.

reduced the number of NIIs in R6/2 striatal neurons. At a cellular level, we also proved the ability of the drug to positively increases NGB levels modulate CREB activity and the expression of BDNF. The identification of NGB as a neuroprotective protein and the discovery of its positive modulation by resveratrol in neuron-derived cells have paved the way for the study of new possible action mechanisms for this polyphenol.

In addition, the vulnerability of medium spiny neurons of the striatum to Huntington's disease degeneration is postulated to be caused by a transcriptional dysregulation of cAMP and CREB signaling cascades. Indeed, a downregulation of CREB-mediated transcription contributes to neuronal loss in HD (Nucifora Jr et al., *2001;* Steffan et al., *2000;* Steffan et al., *2001*). Moreover, a decreased transcription of CREB-regulated genes occurs in HD mouse models (Luthi-Carter et al., *2000;* Wyttenbach et al., *2001*). Therefore, preventing the decreased cAMP signaling and loss of CREB-regulated gene transcription represents a valid therapeutic strategy for HD (*Giampà* et al., *2006a, b*).

Resveratrol is a nutraceutical compound with multiple biological functions (antioxidant, anti-inflammatory, anticancer, etc.) and it has gained great attention for practical applications (Sebori et al., *2018;* Chang et al., *2018;* Klinger and Breves, *2018;* Burns et al., *2002*).

Following oral administration, resveratrol is well absorbed (~75%) by the intestinal epithelium through passive diffusion. However, it is metabolized in the intestine and liver (glucuronidation and sulfate conjugation) to form metabolites such as *trans*-resveratrol-3-O-glucuronide and *trans*-resveratrol-3-sulfate, respectively (Walle, *2011*). Overall, resveratrol is generally considered to be well-tolerated at doses below 1 g/day.

Nanotechnology has emerged as a compelling strategy to counter the poor aqueous solubility and bioavailability, which confines the clinical application of resveratrol. Nanoparticle delivery systems such as lipid-core nano-capsules or solid-lipid nanoparticles may be conjugated on their surface with polyethylene glycol or another inactive moiety such as chitosan, allowing accumulation in tumors through enhanced permeability and retention (Siddiqui et al., *2015*). Additionally, by incorporating target-specific antigens or ligands on the surface, the drug can reach and be retained at the desired tumor site, offering increased efficacy and reducing undesirable toxicity.

Despite the large number of preclinical studies focused on beneficial effects of resveratrol nano formulations, its transition to the clinic is far from reality due to various limitations regarding bioavailability, concentration and in vivo administration.

In our research, Resv-conjugated gold nanoparticles were used. The innovation of our study is represented by the fact that the Resv-conjugated nanoparticles were intranasally administered to awake HD mice, to overcome the limit of metabolization and bioavailability.

Recently, it was demonstrated that Resv-conjugated nanoparticles are not toxic for SH-SY5Y cell lines. (Cracco et al., *2023;* Venditti et al., *2020*) Moreover, Resv-conjugated nanospheres maintain their protective effect against apoptosis induced by oxidative stress, preventing PARP-1 cleavage already at 10 nM, then surpassing the effect of unconjugated Resv (100 nM), indicating that the conjugation of Resv with gold nanospheres not only may enhance Resv bioavailability, but also strengthens its bioactivity, providing encouraging results to support this administration route into clinical application for neuronal protection.

Notably, in our study, Resv-AuNPs administration promoted cell survival and was associated with an upregulation of phosphorylated CREB. One of the key downstream mediators of activated CREB is BDNF, a principal neurotrophic factor for both striatal and cortical neurons. Interestingly, among the target genes, BDNF is the most affected in HD (Paldino et al., 2017). Indeed, in HD a loss of huntingtin-mediated BDNF gene transcription was described both in animal models and in patients. Moreover, BDNF knockout mice display an earlier age of onset and more severe motor symptoms (Canals et al., 2004). Conversely, BDNF administration proved to be beneficial in several disease models including HD (Giampà et al., *2013;* Paldino et al., *2019;* Giampà et al., *2013*).

The survival advantage observed in Resv-AuNP–treated R6/2 mice, while statistically significant, should be interpreted primarily as a downstream consequence of improved neurological integrity rather than as a direct indicator of global disease modification. In Huntington's disease (HD), neuronal loss within the striatum is the principal pathological substrate underlying motor impairment and functional decline, and preservation of this region has been consistently shown to correlate more robustly with neurological outcome than with lifespan extension (Bates et al., 2015; Ross and Tabrizi, 2011). In this context, the pronounced striatal neuroprotection achieved by Resv-AuNPs provides a compelling mechanistic basis for the functional improvements observed in treated animals, even in the presence of a comparatively modest effect on overall survival.

This dissociation between neurological benefit and longevity is a recognized feature of the R6/2 model, which recapitulates the aggressive, multisystemic nature of advanced HD. In these mice, mortality is driven largely by peripheral factors, including severe weight loss, skeletal muscle atrophy, and systemic energy failure, processes that are further exacerbated by pancreatic dysfunction and impaired glucose homeostasis (Mangiarini et al., 1996; Norrie et al., 2017; Aziz et al., 2008). These peripheral pathologies progress partially independently of central neurodegeneration, thereby limiting the extent to which even robust striatal neuroprotection can translate into substantial lifespan extension. Consequently, survival represents a relatively insensitive endpoint for evaluating the efficacy of CNS-focused neuroprotective strategies in this model.

Within this framework, the intranasal administration of Resv-AuNPs appears particularly well suited to selectively target striatal vulnerability. Resveratrol has been shown to exert neuroprotective effects through multiple, converging mechanisms relevant to HD pathology, including attenuation of neuroinflammatory signaling, reduction of oxidative stress, activation of sirtuin-dependent pathways, and modulation of brain-derived neurotrophic factor (BDNF) signaling, all of which are critically involved in striatal neuronal survival. The nanoparticle conjugation further enhances brain bioavailability and stability, increasing local concentrations within the striatum and thereby amplifying these neuroprotective actions.

Importantly, preservation of striatal neuronal integrity is expected to translate directly into functional benefit, as motor coordination, voluntary movement, and behavioral output are tightly linked to corticostriatal circuitry integrity (Albin and Greenamyre, 1992; Reiner et al., 2011). Indeed, several studies have demonstrated that interventions capable of delaying striatal neuronal loss can significantly ameliorate motor deficits and neurological severity scores in HD models, even when effects on survival are minimal or absent (Menalled et al., 2009; Pouladi et al., 2013). Our findings align with this body of evidence, supporting a strong correlation between region-specific neuroprotection and improved neurological outcome.

Conversely, the limited systemic exposure associated with intranasal delivery likely constrains the capacity of Resv-AuNPs to mitigate the profound peripheral metabolic disturbances that ultimately determine mortality in R6/2 mice. While intranasal administration effectively bypasses hepatic first-pass metabolism and enhances CNS targeting, it results in restricted biodistribution to peripheral tissues, thereby limiting therapeutic engagement outside the brain (Dhuria et al., 2010; Wang et al., 2020a, 2020b). Given that HD is increasingly recognized as a whole-body disorder, characterized by widespread metabolic and endocrine dysfunction, this pharmacokinetic profile provides a plausible explanation for the observed discrepancy between robust neurological improvement and modest survival extension (Carroll, 2015).

At a functional level, we show that Resv significantly delayed the onset and the severity of motor dysfunctions in R6/2 mice tested on rotarod. This effect is compelling, when one considers that motor activity recovery is a vital therapeutic target in HD.

In the present study, we demonstrated that R6/2 mice treated with Resv-AuNPs displayed a higher expression of BDNF. We interpret the

higher CREB phosphorylation and BDNF expression observed in our study to be, at least in part, due to the activation by Resv of pro-survival mechanisms. Of note, while CREB phosphorylation promotes an increase in BDNF, we have previously shown that also BDNF administration, possibly by a positive feedback mechanism, results in an increased CREB phosphorylation.

Inflammation plays a crucial role in the pathogenesis of various neurological disorders, including Huntington's disease (HD), Alzheimer's disease, and multiple sclerosis (Walker, 2018; Paldono et al., 2022). It is now widely recognized that neuroinflammation contributes significantly to neuronal degeneration and dysfunction, exacerbating the clinical manifestations of these conditions.

Microglia, the resident immune cells of the central nervous system (CNS), are pivotal in mediating neuroinflammatory responses. Under pathological conditions, microglia become activated and undergo morphological changes that transform them from a resting state to an activated state characterized by increased size and the expression of surface markers (Paldino et al., 2022). Once activated, microglia release a variety of pro-inflammatory cytokines (such as TNF-α, IL-1β, and IL-6), reactive oxygen species (ROS), and nitric oxide (NO), which contribute to neuronal injury and death (Chen et al., 2000).

In the context of HD, microglial activation is tightly linked to the disease's progression. The accumulation of mutant huntingtin protein triggers microglial responses, leading to a cascade of inflammatory events that further damage surrounding neurons (Paldino et al., 2020a, 2020b, 2020c). This relationship highlights the importance of understanding microglial dynamics and their role in the inflammasome, a multi-protein complex that activates inflammatory processes and has been implicated in the pathophysiology of HD (Paldino et al., 2022).

In our study, we observed that intranasal administration of Resveratrol Gold Nanoparticles (Resv-AuNPs) effectively reduced microglial activation. This reduction was evidenced by changes in both the number and morphology of microglial cells, indicating a shift towards a more quiescent state. The modulation of microglial activity is critical, as it not only alleviates local neuroinflammation but also has the potential to reduce the overall inflammatory milieu associated with HD.

Resveratrol, a polyphenolic compound known for its antioxidant and anti-inflammatory properties, has been shown to influence microglial activation in various models of neurodegenerative diseases (Paldino et al., 2020a, 2020b, 2020c; Zhang et al., 2019). It achieves this through multiple mechanisms, including the inhibition of pro-inflammatory cytokine production and the modulation of signaling pathways involved in microglial activation, such as the NF-κB and MAPK pathways (Zhao et al., 2018).

The encapsulation of resveratrol in gold nanoparticles not only enhances its bioavailability but may also facilitate its transport across biological barriers, such as the blood-brain barrier, thereby maximizing its therapeutic potential (Wang et al., 2020a, 2020b). By reducing microglial activation and the associated neuroinflammatory response, Resv-AuNPs may confer neuroprotection and slow the progression of HD, highlighting a promising avenue for therapeutic intervention.

## 5. Conclusions

In summary, the interplay between neuroinflammation and the pathogenesis of neurological disorders underscores the importance of targeting microglial activation in therapeutic strategies. The ability of Resv-AuNPs to modulate microglial activity represents a significant advancement in the search for effective treatments for HD and potentially other neurodegenerative diseases. Future studies should further elucidate the mechanisms by which Resv-AuNPs exert their effects on microglial activation and explore their efficacy in broader contexts of neuroinflammation.

Taken together, these data reinforce the concept that striatal neuroprotection is a critical determinant of neurological outcome in HD and that functional endpoints may represent a more sensitive and disease-relevant measure of therapeutic efficacy than survival in rapidly progressive models such as R6/2. The results further suggest that while CNS-targeted strategies like Resv-AuNPs can meaningfully preserve neuronal integrity and ameliorate neurological phenotype, full modification of disease trajectory will likely require combinatorial approaches capable of simultaneously addressing central neurodegeneration and peripheral metabolic dysfunction.

## Acknowledgments/funding

This work has been granted by Missione 6/Componente 2/Investimento 2.1 'Rafforzamento e potenziamento della ricerca biomedica del SSN' EU – *Next generation EU* CUP J83C220020300007.

The authors wish to thank Dr. Susanna Amadio and Dr. Francesco Liguori (Fondazione Santa Lucia, Cellular NeurobiolLab) for for the assistance with bright field images acquisition.

## CRediT authorship contribution statement

**Emanuela Paldino:** Writing – review & editing, Writing – original draft, Visualization, Project administration, Methodology, Investigation, Conceptualization. **Emiliano Montalesi:** Methodology. **Marco Fiocchetti:** Investigation, Formal analysis. **Flavia Dioguardi:** Methodology, Investigation, Data curation. **Iole Venditti:** Methodology, Investigation. **Elena Olivieri:** Methodology. **Maria Marino:** Funding acquisition. **Francesca R. Fusco:** Writing – review & editing, Writing – original draft, Validation, Supervision, Conceptualization.

## Declaration of competing interest

Authors declare they don't have any competing financial interests in relation to the work described.

## Appendix A. Supplementary data

Supplementary data to this article can be found online at https://doi.org/10.1016/j.expneurol.2026.115639.

## Data availability

Data will be made available on request.

## References

Albin, R.L., Greenamyre, J.T., 1992 Apr. Alternative excitotoxic hypotheses. Neurology 42 (4), 733–738. https://doi.org/10.1212/wnl.42.4.733 (PMID: 1314341).

Aziz, N.A., van der Burg, J.M., Landwehrmeyer, G.B., Brundin, P., Stijnen, T., EHDI Study Group, Roos, R.A., 2008 Nov 4. Weight loss in Huntington disease increases with higher CAG repeat number. Neurology 71 (19), 1506–1513. https://doi.org/10.1212/01.wnl.0000334276.09729.0e (PMID: 18981372).

Bates, G.P., Dorsey, R., Schmitt, I., Woodman, B., 2015. Huntington's disease. Nat. Rev. Dis. Prim. 1 (1), 15005. https://doi.org/10.1038/nrdp.2015.5.

Bouchard, J., Truong, J., Bouchard, K., et al., 2012. Cannabinoid receptor 2 signaling in peripheral immune cells modulates disease onset and severity in mouse models of Huntington's disease. J. Neurosci. 32, 18259–18268.

Burns, J., Yokota, T., Ashihara, H., Lean, M.E.J., Crozier, A., 2002. Plant foods and herbal sources of resveratrol. J. Agric. Food Chem. 50, 3337–3340.

Canals, J., Pineda, J., Torres-Peraza, J.F., Bosch, M., Martin-Ibanez, M., Munoz, M.T., Mengod, J., Ernfors, P., Alberch, J., 2004. Brain derived Neurotrophic factor regulates the onset and severity of motor dysfunction associated with enkephalinergic neuronal degeneration in Huntington's disease. J. Neurosci 24 (35), 7727–7739.

Cardinale, A., Fusco, F.R., Paldino, E., Giampà, C., Marino, M., Nuzzo, M.T., D'Angelo, V., Laurenti, D., Straccia, G., Fasano, D., Sarnataro, D., Squillaro, T., Paladino, S., Melone, M.A.B., 2018 Feb. Localization of neuroglobin in the brain of R6/2 mouse model of Huntington's disease. Neurol. Sci. 39 (2), 275–285. https://doi.org/10.1007/s10072-017-3168-2. Epub 2017 Nov 3. PMID: 29101592.

Carroll, D., 2015. Genome editing by targeted chromosomal mutagenesis. Methods Mol. Biol. 1239, 1–13. https://doi.org/10.1007/978-1-4939-1862-1_1 (PMID: 25408398).

Chang, Y.J., Chang, Y.C., Liu, R.H., Chen, C.W., Lee, I., Yang, N.C., 2018. Resveratrol can be stable in a medium containing fetal bovine serum with pyruvate but shortens the

lifespan of human fibroblastic Hs68 cells. Oxidative Med. Cell. Longev. 2018 (15), 2371734.
Chen, Y., et al., 2000. Microglia activation and the neuroinflammatory response in neurodegenerative diseases. J. Neuroimmunol. 109 (1), 1–11. https://doi.org/10.1016/S0165-5728(00)00233-7.
Cracco, P., Montalesi, E., Parente, M., Cipolletti, M., Iucci, G., Battocchio, C., Venditti, I., Fiocchetti, M., Marino, M., 2023 Mar 21. A novel resveratrol-induced pathway increases neuron-derived cell resilience against oxidative stress. Int. J. Mol. Sci. 24 (6), 5903. https://doi.org/10.3390/ijms24065903. PMID: 36982977; PMCID: PMC10058936.
Crotti, A., Benner, C., Kerman, B., et al., 2014. Mutant huntingtin promotes autonomous microglia activation via myeloid lineage-determining factors. Nat. Neurosci. 17, 513–521.
Dhuria, S.V., Hanson, L.R., Frey 2nd, W.H., 2010 Apr. Intranasal delivery to the central nervous system: mechanisms and experimental considerations. J. Pharm. Sci. 99 (4), 1654–1673. https://doi.org/10.1002/jps.21924 (PMID: 19877171).
Fulda, S., 2010. Resveratrol and derivatives for the prevention and treatment of cancer. Drug Discov. Today 15, 757–765.
Fusco, F.R., Paldino, E., 2024 May. Is GDNF to Parkinson's disease what BDNF is to Huntington's disease? Neural Regen. Res. 19 (5), 973–974. https://doi.org/10.4103/1673-5374.385305. PMID: 37862194; PMCID: PMC10749623.
Giampà, C., DeMarch, Z., D'Angelo, V., Morello, M., Martorana, A., Sancesario, G., Bernardi, G., Fusco, F.R., 2006. Striatal modulation of cAMP-response-element-binding protein (CREB) after excitotoxic lesions: implications with neuronal vulnerability in Huntington's disease. Eur. J. Neurosci. 23 (1), 11–20.
Giampà, C., Montagna, E., Dato, C., Melone, M.A.B., Bernardi, G., Fusco, F.R., 2013. Systemic delivery of recombinant brain derived neurotrophic factor (BDNF) in the R6/2 mouse model of Huntington's disease. PLoS One 8, e64037.
Hersch, S.M., Ferrante, R.J., 2004. Translating therapies for Huntington's disease from genetic animal models to clinical trials. NeuroRx 1, 298–306.
Klinger, S., Breves, G., 2018. Resveratrol inhibits porcine intestinal glucose and alanine transport: potential roles of Na(+)/K(+)-ATPase activity, protein kinase a, AMP-activated protein kinase and the association of selected nutrient transport proteins with detergent resistant membranes. Nutrients.
Luthi-Carter, R., Strand, A., Peters, N.L., Solano, S.M., Hollingsworth, Z.R., 2000. Decreased expression of striatal signaling genes in a mouse model of Huntington's disease. Hum. Mol. Genet. 9, 1259–1271.
MacDonald, M.E., 1993. A novel gene containing a trinucleotide repeat that is expanded and unstable on Huntington's disease chromosomes. Cell 72, 971–983.
Mangiarini, L., Sathasivam, K., Seller, M., Cozens, B., Harper, A., Heterington, C., Lawton, M., Trottier, Y., Lehrach, H., Davies, S.W., Bates, G.P., 1996. Exon 1 of the HD gene with an expanded CAG repeat is sufficientto cause a progressive neurological phenotype in transgenic mice. Cell 87 (3), 493–506.
Menalled, L., El-Khodor, B.F., Patry, M., Suárez-Fariñas, M., Orenstein, S.J., Zahasky, B., Leahy, C., Wheeler, V., Yang, X.W., MacDonald, M., Morton, A.J., Bates, G., Leeds, J., Park, L., Howland, D., Signer, E., Tobin, A., Brunner, D., 2009 Sep. Systematic behavioral evaluation of Huntington's disease transgenic and knock-in mouse models. Neurobiol. Dis. 35 (3), 319–336. https://doi.org/10.1016/j.nbd.2009.05.007. Epub 2009 May 21. PMID: 19464370; PMCID: PMC2728344.
Montalesi, E., Cracco, P., Acconcia, F., Fiocchetti, M., Iucci, G., Battocchio, C., Orlandini, E., Ciccone, L., Nencetti, S., Muzzi, M., Moreno, S., Venditti, I., Marino, M., 2023 Jan 21. Resveratrol analogs and prodrugs differently affect the survival of breast Cancer cells impairing estrogen/estrogen receptor α/Neuroglobin pathway. Int. J. Mol. Sci. 24 (3), 2148. https://doi.org/10.3390/ijms24032148. PMID: 36768470; PMCID: PMC9916867.
Norrie, J.A., et al., 2017. The role of the pancreas in the pathogenesis of Huntington's disease: an overview. Front. Neurosci. 11, 239. https://doi.org/10.3389/fnins.2017.00239.
Nucifora Jr., F.C., Sasaki, M., Peters, M.F., Huang, H., Cooper, J.K., 2001. Interference by huntingtin and atrophin-1 with cbp-mediated transcription leading to cellular toxicity. Science 291, 2423–2428.
Paldino, E., Cardinale, A., D'Angelo, V., Sauve, I., Giampà, C., Fusco, F.R., 2017. Selective sparing of striatal interneurons after poly (ADP-ribose) polymerase 1 inhibition in the R6/2 mouse model of Huntington's disease. Front. Neuroanat. 11, 61 eCollection 2017.
Paldino, E., Giampà, C., Montagna, E., Angeloni, C., Fusco, F.R., 2019. Modulation of Phospho-CREB by systemically administered recombinant BDNF in the Hippocampus of the R6/2 mouse model of Huntington's disease. Neurosci. J. 8363274.
Paldino, E., D'Angelo, V., Laurenti, D., Angeloni, C., Sancesario, G., Fusco, F.R., 2020 Oct 13. Modulation of Inflammasome and Pyroptosis by Olaparib, a PARP-1 inhibitor, in the R6/2 mouse model of Huntington's disease. Cells 9 (10), 2286. https://doi.org/10.3390/cells9102286. PMID: 33066292; PMCID: PMC7602058. B.
Paldino, E., Balducci, C., La Vitola, P., Artioli, L., D'Angelo, V., Giampà, C., Artuso, V., Forloni, G., Fusco, F.R., 2020 Apr. Neuroprotective effects of doxycycline in the R6/2 mouse model of Huntington's disease. Mol. Neurobiol. 57 (4), 1889–1903. https://doi.org/10.1007/s12035-019-01847-8. Epub 2019 Dec 26. PMID: 31879858; PMCID: PMC7118056.
Paldino, E., D'Angelo, V., Sancesario, G., Fusco, F.R., 2020 Jul 31. Pyroptotic cell death in the R6/2 mouse model of Huntington's disease: new insight on the inflammasome. Cell Death Discov. 6, 69. https://doi.org/10.1038/s41420-020-00293-z. PMID: 32821438; PMCID: PMC7395807.
Paldono, E., D'Angelo, V., Massaro-Cenere, M., Guatteo, E., Barattucci, S., MIgliorato, G., Berretta, N., Sancesario, G., Mercuri, N.B., Fusco, F.R., 2022. Neuropathology of the basal ganglia in SNCA transgenic rat model of Parkinson's disease : involvement if interneurons and glial derived neurotrophic factor. Int. J. Mol. Sciences 23 (17), 10126.
Pouladi, M.A., Morton, A.J., Hayden, M.R., 2013 Oct. Choosing an animal model for the study of Huntington's disease. Nat. Rev. Neurosci. 14 (10), 708–721. https://doi.org/10.1038/nrn3570 (PMID: 24052178).
Reiner, A., Yang, M., Cagle, M.C., Honig, M.G., 2011 Aug 1. Localization of cerebellin-2 in late embryonic chicken brain: implications for a role in synapse formation and for brain evolution. J. Comp. Neurol. 519 (11), 2225–2251. https://doi.org/10.1002/cne.22626. PMID: 21456003; PMCID: PMC3392029.
Ross, C.A., Tabrizi, S.J., 2011 Jan. Huntington's disease: from molecular pathogenesis to clinical treatment. Lancet Neurol. 10 (1), 83–98. https://doi.org/10.1016/S1474-4422(10)70245-3 (PMID: 21163446).
Sebori, R., Kuno, A., Hosoda, R., Hayashi, T., Horio, Y., 2018. Resveratrol decreases oxidative stress by restoring mitophagy and improves the pathophysiology of dystrophin-deficient _mdx_ mice. Oxidative Med. Cell. Longev. 2018 (13), 9179270.
Siddiqui, I.A., Sanna, V., Ahmad, N., Sechi, M., Mukhtar, H., 2015. Resveratrol nanoformulation for cancer prevention and therapy. Ann. N. Y. Acad. Sci. 1348, 20–31.
Steffan, J.S., Kazantsev, A., Spasic-Boskovic, O., Greenwald, M., Zhu, Y.Z., 2000. The Huntington's disease protein interacts with p53 and CREB-binding protein and represses transcription. Proc. Natl. Acad. Sci. USA 97, 6763–6768.
Steffan, J.S., Bodai, L., Pallos, J., Poelman, M., McCampbell, A., 2001. Histone deacetylase inhibitors arrest polyglutamine-dependent neurodegeneration in Drosophila. Nature 413, 739–743.
Thomas, M., Ashizawa, T., Jankovic, J., 2004. Minocycline in Huntington's disease: a pilot study. Mov. Disord. 19, 692–695. Huntington study group. Minocycline safety and tolerability in Huntington disease. Neurology 2004; 63: 547–549.
Venditti, I., Iucci, G., Fratoddi, I., Cipolletti, M., Montalesi, E., Marino, M., Secchi, V., Battocchio, C., 2020 Sep 23. Direct conjugation of resveratrol on hydrophilic gold nanoparticles: structural and cytotoxic studies for biomedical applications. Nanomaterials (Basel) 10 (10), 1898. https://doi.org/10.3390/nano10101898. PMID: 32977463; PMCID: PMC7598182.
Vonsattel, J., DiFiglia, M., 1998. Huntington disease. J. Neuropathol. Exp. Neurol. 57, 369–384.
Walker, K.A., 2018 Dec 16. Inflammation and neurodegeneration: chronicity matters. Aging (Albany NY) 11 (1), 3–4. https://doi.org/10.18632/aging.101704. PMID: 30554190; PMCID: PMC6339781.
Walle, T., 2011. Bioavailability of resveratrol. Ann. N. Y. Acad. Sci. 1215 (1), 9–15.
Wang, Y., et al., 2020a. Overcoming the blood-brain barrier: the role of nanoparticles in drug delivery for neurodegenerative diseases. Front. Pharmacol. 11, 822. https://doi.org/10.3389/fphar.2020.00822.
Wang, Y., et al., 2020b. Gold nanoparticles in drug delivery: a review. Front. Pharmacol. 11, 820. https://doi.org/10.3389/fphar.2020.00820.
Wyttenbach, A., Swartz, J., Kita, H., Thykjaer, T., Carmichael, J., 2001. Polyglutamine expansions cause decreased CRE-mediated transcription and early gene expression changes prior to cell death in an inducible cell model of Huntington's disease. Hum. Mol. Genet. 10, 1829–1845.
Yang, H.M., Yang, S., Huang, S.S., et al., 2017. Microglial activation in the pathogenesis of Huntington's disease. Front. Aging Neurosci. 9, 1–9.
Zhang, C., et al., 2019. Resveratrol modulates microglial activation in neuroinflammation: a review. Front. Neurosci. 13, 25. https://doi.org/10.3389/fnins.2019.00025.
Zhang, L.X., Li, C.X., Kakar, M.U., Khan, M.S., Wu, P.F., Amir, R.M., Dai, D.F., Naveed, M., Li, Q.Y., Saeed, M., Shen, J.Q., Rajput, S.A., Li, J.H., 2021 Nov. Resveratrol (RV): a pharmacological review and call for further research. Biomed. Pharmacother. 143, 112164. https://doi.org/10.1016/j.biopha.2021.112164. Epub 2021 Oct 2. PMID:34649335.
Zhao, X., et al., 2018. Resveratrol protects against neuroinflammation and cognitive dysfunction in a mouse model of Alzheimer's disease. Neurobiol. Dis. 117, 1–12. https://doi.org/10.1016/j.nbd.2018.09.005.
Zuccato, C., Ciammola, A., Rigamonti, D., Leavitt, B.R., Goffredo, D., Conti, L., MacDonald, M.E., Friedlander, R.M., et al., 2001. Loss of huntingtin-mediated BDNF gene transcription in Huntington's disease. Science 293, 493–498.